An assessment of CFD applied to steady flow in a planar diffuser upstream of an automotive catalyst

Porter, S. , Mat Yamin, A.K. , Aleksandrova, S. , Benjamin, S.F. , Roberts, C.A. and Saul, J.

2014-01-2588
Published 10/13/2014

doi:10.4271/2014-01-2588
saeeng.saejournals.org

An Assessment of CFD Applied to Steady Flow in a Planar Diffuser Upstream of an Automotive Catalyst Monolith

Sophie Porter
Coventry Univ.

Ahmad Kamal Mat Yamin
Universiti Teknikal Malaysia Melaka

Svetlana Aleksandrova, Stephen Benjamin, Carol A. Roberts, and Jonathan Saul
Coventry Univ.

ABSTRACT

Flow maldistribution across automotive exhaust catalysts significantly affects their conversion efficiency. Flow behaviour can be predicted using computational fluid dynamics (CFD). This study investigates the application of CFD to modelling flow in a 2D system consisting of a catalyst monolith downstream of a wide-angled planar diffuser presented with steady flow. Two distinct approaches, porous medium and individual channels, are used to model monoliths of length 27 mm and 100 mm. Flow predictions are compared to particle image velocimetry (PIV) measurements made in the diffuser and hot wire anemometry (HWA) data taken downstream of the monolith. Both simulations compare favourably with PIV measurements, although the models underestimate the degree of mixing in the shear layer at the periphery of the emerging jet. Tangential velocities are predicted well in the central jet region but are overestimated elsewhere, especially at the closest measured distance, 2.5 mm from the monolith. The individual channels model is found to provide a more consistently accurate velocity profile downstream of the monolith. Maximum velocities, on the centre line and at the secondary peak near to the wall, are reasonably well matched for the cases where the flow is more maldistributed. Under these conditions, a porous medium model remains attractive because of low computational demand.

CITATION: Porter, S., Mat Yamin, A., Aleksandrova, S., Benjamin, S. et al., "An Assessment of CFD Applied to Steady Flow in a Planar Diffuser Upstream of an Automotive Catalyst Monolith," *SAE Int. J. Engines* 7(4):2014, doi:10.4271/2014-01-2588.

INTRODUCTION

Catalytic converters are widely used in the automotive industry in order to reduce harmful exhaust emissions and conform to emission regulations. For optimum conversion efficiency, uniform flow is required across the monolith. Computational fluid dynamics (CFD) is increasingly being used to assess the flow distribution of different design concepts; it is therefore necessary that predictions of flow behaviour offered by CFD are reliable and of sufficient accuracy.

The catalyst is typically a ceramic monolith structure comprised of many parallel channels of square cross-section and small hydraulic diameter (~1 mm). The precious metals of the catalyst are embedded in a thin washcoat applied to the channel walls, thus providing a large surface area for reaction of exhaust pollutants. The size and shape of monolith depends on vehicle size and packaging constraints, however a typical passenger vehicle monolith would have a circular or oval cross-section and a cell density between 31 and 140 cells/cm^2.

Due to space constraints, wide-angled diffusers are used to connect the exhaust pipe to the front face of the catalyst. This results in flow separation at the diffuser inlet and a non-uniform flow distribution within the monolith.

Modelling the flow is challenging. The model should not only adequately simulate the flow in the diffuser but also account for the pressure loss associated with the monolith itself. One approach would be to solve the flow field both within the diffuser and in each of the individual channels. This is computationally demanding as it requires discretising the flow domain over several thousand channels. An alternative approach, widely used, is to treat the monolith as a porous medium or equivalent continuum. This reduces the computational effort but requires an accurate prescription of the monolith resistance. A common assumption is that this can be adequately described by losses associated with unidirectional flow in the channels. These can be obtained from theoretical considerations or can be measured directly on a flow rig. Benjamin et al. [1] found that using this approach for

axi-symmetric systems resulted in CFD under-estimating the degree of flow maldistribution. This was attributed to an inaccurate prescription of losses at locations in the monolith where the flow approached the channels obliquely.

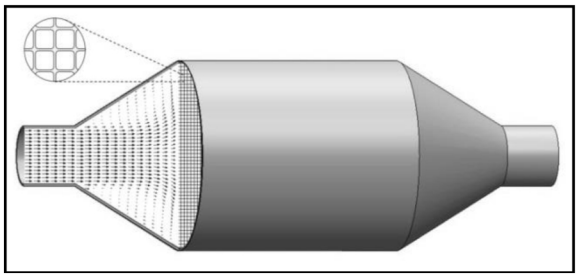

Figure 1. Schematic of flow in a catalyst assembly.

This can be illustrated by Figure 1, which shows an example of flow through an axi-symmetric wide-angled diffuser placed upstream of a monolith. The flow separates at the inlet, producing a confined jet that traverses the diffuser. Near the monolith the jet decelerates and spreads radially. Part of the flow enters the channels, the rest feeds the recirculating gas located between the jet and the diffuser wall. The net effect is that the flow entering the monolith is maldistributed, with the highest velocity occurring in the channels near the centre of the monolith. On the centre-line flow enters the channels axially, whereas at larger radial distances it approaches them obliquely. This can cause flow separation at the channel entrance, especially at high incidence, and hence an increased resistance at these locations. The radial flow stagnates as it approaches the diffuser wall near the front face of the monolith, causing a rise in pressure and encouraging flow through the outermost channels. This results in secondary velocity peaks for channels close to the wall.

Losses due to oblique entry have been measured by Quadri et al. [2] and Persoons et al. [3]. Küchemann and Weber [4] derived an expression for this pressure loss, given in Eq. (1), based on considerations of oblique entry into flat plate heat exchangers.

$$\Delta P_{obl} = \frac{\rho v^2}{2} \qquad (1)$$

Here ρ denotes fluid density and v the transverse velocity component of flow upon entry into the heat exchanger. Incorporating Eq. (1) into CFD simulations, Benjamin et al. [1] achieved much-improved maximum velocity predictions; however, the secondary peaks were over-predicted. This was attributed to very high levels of resistance at high incidence, promoting increased flow towards the outer channels. A critical angle approach was therefore proposed by Quadri et al. [2], where the pressure losses were capped at higher angles of attack. For a given critical angle α_c, the pressure loss was assumed to satisfy

$$\Delta P_{obl} = \begin{cases} \frac{\rho v^2}{2}, & \alpha < \alpha_c \\ \frac{\rho v_c^2}{2}, & \alpha \geq \alpha_c \end{cases} \qquad (2)$$

where α denotes the angle of attack and v_c the transverse velocity component of flow entering at α_c. This improved predictions of the velocity distribution, although the distribution away from the centre-line was shown to be quite sensitive to the chosen value of the critical angle.

These studies compared predictions with velocity measurements at the monolith exit and hence implicitly assumed that predictions within the diffuser were correct. Development of optical methods such as particle image velocimetry has now enabled measurement of the flow field upstream of the monolith. Breuer et al. [5] used PIV and hot wire anemometry downstream of a catalytic converter to validate CFD, while Turner et al. [6] used PIV for the validation of CFD applied to flow in the inlet diffuser upstream of a diesel particulate filter. Quadri et al. [7] measured velocity profiles upstream and downstream of monoliths for a planar geometry with steady flow. Mat Yamin et al. [8] obtained similar data under both steady and pulsating flow. This paper uses the steady flow data from [8] and extra measurements performed with a fitted sleeve to compare porous medium model predictions with measurements both within the diffuser and in the monolith (as measured downstream). The planar geometry provides full optical access in the diffuser and permits detailed comparisons to be made. Measurements downstream of the monolith also provide the opportunity to assess the validity of the pressure loss expressions discussed previously.

The porous medium approach is computationally efficient but requires prescription of the pressure loss as discussed above. A model which includes the geometry of all the monolith channels provides a detailed representation of the geometry and avoids the need to prescribe these losses a-priori. However it is achieved at the expense of a high computational demand. The 2D planar geometry described in [8], however, does provide the opportunity of assessing this type of model by only requiring the modelling of channels across a section of the catalyst. Such a model is also described in this paper and is compared with the porous medium approach.

METHODOLOGY

Experimental Data Collection

Figure 2 shows a schematic diagram of the isothermal flow rig used for steady state flow measurements. The experimental set-up is presented by Mat Yamin [8, 9] and is reiterated here.

The high pressure line supplies air through a viscous flow meter into the flow rig (1) where a plenum (2) with flow straightener (3) and axisymmetric nozzle (4) leads to a pulse generator (5). Measurements of non-pulsating flow, used in the current study, were obtained by fixing the rotor of the pulse generator in a fully open position. Air then flows through another flow straightener (6) and past a resonator box (7), installed to shape pulses during pulsating flow studies. A particle generator (9) supplies seeding to a second plenum (8) with flow straightener (10) to minimise any swirl components. A two-dimensional nozzle (11) provides uniform flow to the planar diffuser (12), thus generating well-defined inlet conditions for CFD. The diffuser has inlet dimensions 24 × 96 mm, outlet dimensions 78 × 96 mm, length 48 mm and total included angle of approximately 60°. The diffuser is made of crown glass for optimal optical conditions for PIV. The diffuser outlet attaches to an unwashcoated cordierite monolith (13) of length 27 mm or 100 mm. The monoliths had channel hydraulic diameter 1.12 mm, a nominal cell density of 62 cells/cm^2 and porosity 0.77. An outlet sleeve (14) of length 50 mm minimised any influence from air outside the rig. The sleeve had dimensions 125 × 137 mm and thus provided an expansion at the rear of the monolith. As part of the present investigation a fitted sleeve of the same dimensions as the diffuser outlet was used and HWA profiles were measured at the rear of the monolith. These measurements permitted an assessment of the performance of the models in predicting flow within the monolith and mixing downstream of the monolith.

Flow within the diffuser was measured using a TSI PIV system. A six-jet atomiser at 25 psi produced olive oil droplets of approximately 0.6 μm diameter. A cylindrical lens of −25 mm focal length was combined with a spherical lens of 500 mm to transform the circular beam from a 120 mJ solid-state Nd:YAG laser into an approximately 1 mm thick light sheet at a stand-off distance of 0.5 m to illuminate the seeded flow. A 4-megapixel CCD camera with resolution of 2048 × 2048 pixel (1 pixel = 7.4 μm) was used to capture the flow field. The camera, coupled with a 105 mm lens, was placed 0.8 m from the measurement plane to cover an 80 × 60 mm field of view resulting in a magnification factor of 0.155. An *f* number of 11 enabled a particle image diameter above 2 pixels, therefore avoiding pixel locking. INSIGHT-3G software was used for image processing. The recursive Nyquist method with a 64 × 64 initial grid and a final grid of 32 × 32 pixels yielded 95% valid vectors in each field and vector resolution of 0.76 mm.

Axial velocity profiles at the nozzle exit and downstream of the monolith were obtained using a TSI IFA 300 hot-wire anemometry system. 5 μm platinum-plated tungsten wires (Dantec 55 P11) were calibrated on an automatic TSI 1129 calibration rig. A 1 MHz 4 channel 12 bit A/D converter converted the IFA output voltage (±5 V) to a digital signal to be processed by ThermalPro software.

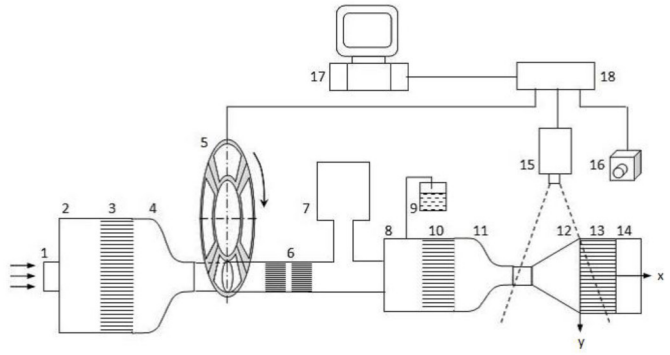

Figure 2. Schematic diagram of 2D isothermal flow rig

CFD Design

Flow simulations were performed using the commercial CFD code Star-CCM+ on a flow domain consisting of a diffuser, substrate and outlet sleeve (Figure 3). Velocity profiles across horizontal and vertical planes at the nozzle exit were found to be acceptably uniform [8], thus flow at the diffuser inlet may be assumed one-dimensional for simulation purposes. Velocity profiles at the monolith exit for various z positions [9] show little variation and symmetry; it is therefore acceptable to model the system as two-dimensional and symmetrical with respect to the plane y=0. The fluid is modelled as a constant density air flow. Reynolds averaged Navier Stokes (RANS) equations are combined with the v^2f turbulence model, proven to improve accuracy for separating flows [10].

The computational method entailed in this study comprises of two distinct approaches to the same problem. The first is the more common method of modelling the monolith as a porous medium with a prescribed resistance. The second technique allows the monolith to retain its solid properties at the channel walls and therefore employs a geometry design inclusive of small, parallel channels through which fluid flows. The model requires a three-dimensional mesh with prism layers at the channels walls. Table 1 compares the computational resources required for each approach. The meshes cited were subject to a mesh independence study, which showed negligible change to solutions for a more refined mesh.

Table 1. Computational resources for CFD models

Model	Porous Medium		Individual Channels	
Monolith length	27 mm	100 mm	27 mm	100 mm
# cells	28,423	47,354	3,962,318	8,824,908

Porous Medium Approach

This model treats the monolith as a porous medium. The axial resistance of the substrate was found from flow rig measurements. A second order polynomial function was fitted to the values of superficial velocity and measured pressure drop. The pressure loss per unit length depends on the viscous resistance coefficient γ and inertial resistance coefficient β and is given by

$$\Delta P/L = \gamma u_s + \beta u_s^2 \quad (3)$$

where u_s denotes superficial velocity in the monolith and L the length of the monolith. Values of β = 14.053 kg/m^4, γ = 734.48 kg/m^{3}s and β = 19.806 kg/m^4, γ = 259.5 kg/m^{3}s are derived for the 27 mm and 100 mm monoliths respectively. The model employs the coefficients γ and β as constants of resistance in the direction of flow. A suitably high coefficient in the y-direction, in this case 10^7, is then fixed in order to ensure unidirectional flow in the monolith. Entrance effects defined by Eqs. (1, 2) are imposed as momentum source functions throughout the length of the monolith and are calculated from velocity data extracted from the simulation 1 mm upstream of the monolith. The flow here is found to have progressed sufficiently to most accurately represent flow behaviour upon entry into the monolith, but is not yet affected by interaction with the monolith face.

Individual Channels Approach

In this case the monolith is modelled as a system of multiple parallel channels. The geometry of the square cells was determined by using the manufacturer's specification. The monoliths used in this study are unwashcoated with porosity 0.77, channel hydraulic diameter 1.12 mm and nominal cell density 62 cells/cm^2. The model geometry, shown in Figures 3 and 4, is three-dimensional; the domain includes half-channel width in the z-direction with half wall thickness. Due to symmetry of the system with respect to y, only half the monolith width is included, with the z-axis on the centre-line of a cell. The diffuser and outlet sleeve are three-dimensional with symmetry with respect to z imposed on xy-planes. Prism layers are included at the channel walls in order to capture developing boundary layers, see Figure 5.

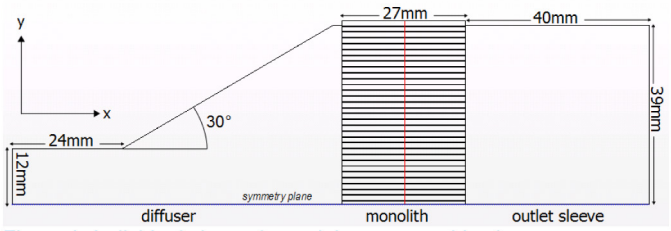

Figure 3. Individual channels model geometry side view

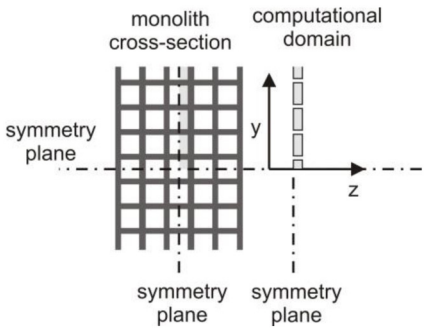

Figure 4. Part-view of cross sectional plane halfway down monolith length for individual channels model

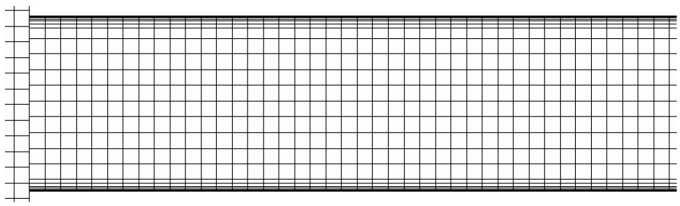

Figure 5. Mesh resolution of channel

Results

Figures 7 and 8 show the axial velocity distribution for each approach. In the diffuser flow characteristics are similar to those described earlier for the case of axi-symmetric assemblies with wide-angled conical diffusers. The flow separates at the inlet to the diffuser, forming a planar jet which spreads rapidly close to the monolith. Large recirculation regions are formed between the jet surface and the diffuser wall. In Figure 7, jets of fluid are visible as the flow leaves the monolith and enters the outlet sleeve. Developing boundary layers are seen in the channels and in particular, the presence of small recirculation bubbles can be seen at the entrance of those channels where the angle of attack is more oblique (Figure 6). None of these features are present in the porous medium model (Figure 8).

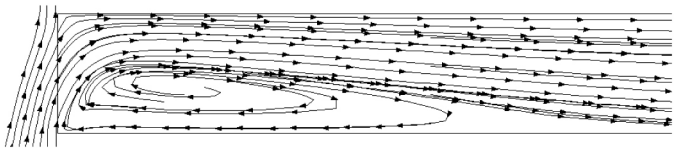

Figure 6. Streamlines at entrance to a channel for individual channels model (symmetry plane) with 27 mm monolith and inlet Re 2 × 10^4

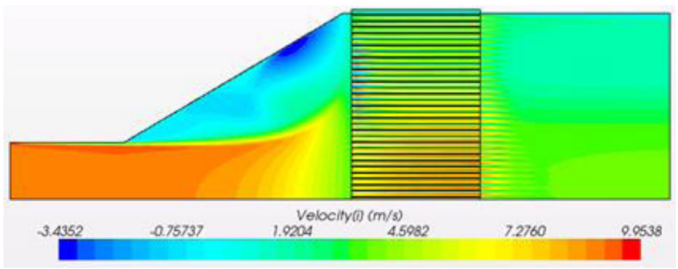

Figure 7. Axial velocity contours for individual channels model (symmetry plane) with 27 mm monolith and inlet Re 2 × 10^4

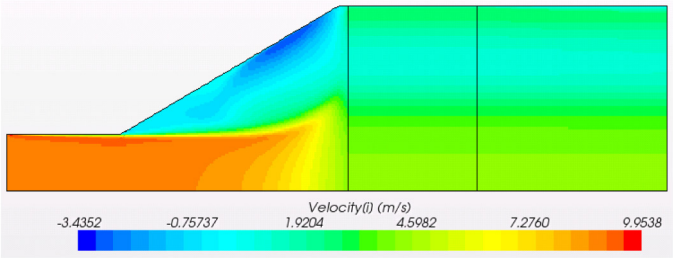

Figure 8. Axial velocity contours for porous medium model with entrance effect with 27 mm monolith and inlet Re 2 × 10^4

Cross-sections of flow in the diffuser are compared for the two simulations and PIV data. Figures 9 and 10 show axial and tangential velocity profiles 10.13 mm, 5.55 mm and 2.5 mm upstream of a 27 mm monolith at two values of Reynolds number (based on inlet diameter and mean velocity). The general features of the profiles reflect the flow structure described above, as shown in Figures 7, 8, 11 and 12. The flow enters the diffuser from the nozzle with a flat velocity profile and separates, forming a jet which traverses the diffuser. The potential core region of the jet is flanked by regions of raised velocity giving rise to characteristic saddle profiles [7, 8]. These are believed to be associated with the effect of the recirculating flow “squeezing” the jet as it emerges into the diffuser. Large recirculation regions are formed in the diffuser between the jet periphery and the wall as evidenced by the negative axial velocities near the wall. As the jet approaches the monolith it decelerates and spreads rapidly (tangential velocity increasing). Results from the single channel and porous medium simulations are very similar which is not unexpected as they differ only in respect to the way the downstream resistance (monolith) is modelled. Both simulations compare favourably with PIV measurements although there are some differences. Both show the characteristic saddle profiles but underestimate the degree of mixing as evidenced by the steeper gradient in the axial profiles in the shear layer at the jet periphery. This leads to an apparent overestimation of the jet “width”, visible in Figures 11 and 12. The tangential velocities are well-predicted in the central jet region but are overestimated elsewhere, especially at the closest measured distance, 2.5 mm from the monolith. This suggests that the predicted angle of incidence of the flow upon entry into the monolith channels may be too high.

Figures 13, 14, 15, 16 show axial velocity profiles 40 mm downstream of the monolith. HWA data obtained with the fitted sleeve is compared with the individual channels approach and the porous medium approach without the entrance effect and with its inclusion. The entrance effect simulations are shown using the $\rho v^2/2$ formulation, one of which also assumes a critical angle $\alpha_c = 69°$. Non-dimensional profiles are obtained by dividing axial velocity u by the mean superficial velocity in the monolith $\bar{U}$. The HWA data is representative of the axial velocity profiles within the monolith. At a distance of 40 mm downstream of the monolith, mixing from the individual jets emerging from the monolith channels (see Figure 7) has proceeded sufficiently to ensure relatively smooth profiles are obtained. The HWA profiles may be compared with the PIV axial profiles measured 2.5 mm upstream of the monolith as shown in Figures 9 and 10. There is clearly a radical restructuring of the flow between the front face of the monolith into the channels themselves. PIV data closer than 2.5 mm to the monolith front face is evidently needed to identify the peripheral secondary velocity peaks recorded downstream. Modelling the flow as it enters the monolith clearly presents a considerable challenge.

Figures 13, 14, 15, 16 show that without inclusion of the entrance effect, for cases with high maldistribution, the flow distribution is predicted to be too uniform, as was the case for axi-symmetric geometries [1]. In particular the maximum velocity is under predicted. This is important as high velocities can lead to premature deactivation of the catalyst and reduced conversion efficiency. Including the entrance effect gives an improved prediction of the maximum velocity. The effect of the critical angle is to modify predictions of the minimum velocity between the peaks and the height of the secondary peaks. These features are sensitive to the value chosen for the critical angle as demonstrated in [2], where a few degrees' difference was shown to significantly alter the secondary peak profiles. Figures 9 and 10 show that it is difficult to predict the oblique entry angle to the required accuracy to confidently simulate these secondary peaks and this would seem to be an inherently limiting factor for the porous medium approach. However the porous medium approach can predict the maximum velocity with acceptable accuracy and, given its computational efficiency, provides an attractive alternative to modelling the individual channels.

Figures 13, 14, 15, 16 show that for the 27 mm monolith the individual channels model predicts the maximum velocities to about the same level of accuracy as the porous medium models and predicts the profile shape somewhere between the porous medium simulations. Hence its overall performance is similar to the porous medium models. The single channel model does produce flatter profiles than the porous medium models for the case of the 100 mm monolith and provides a closer match to the HWA measurements. However, all profiles are relatively flat and model performance is less critical under these conditions.

The effect of the expansion sleeve as used in [8] is to displace the secondary velocity peaks in-board due to mixing in the outermost channels as the flow exits the monolith. The same CFD methodology described earlier has been applied to a geometry featuring this sleeve as shown in Figure 17. Figure 18 shows axial velocity profiles 40 mm downstream for the case of a 27 mm monolith with inlet Re 3 × 10^4. The porous medium approach is seen to poorly predict this lateral displacement of secondary peaks compared to the single channel simulation.

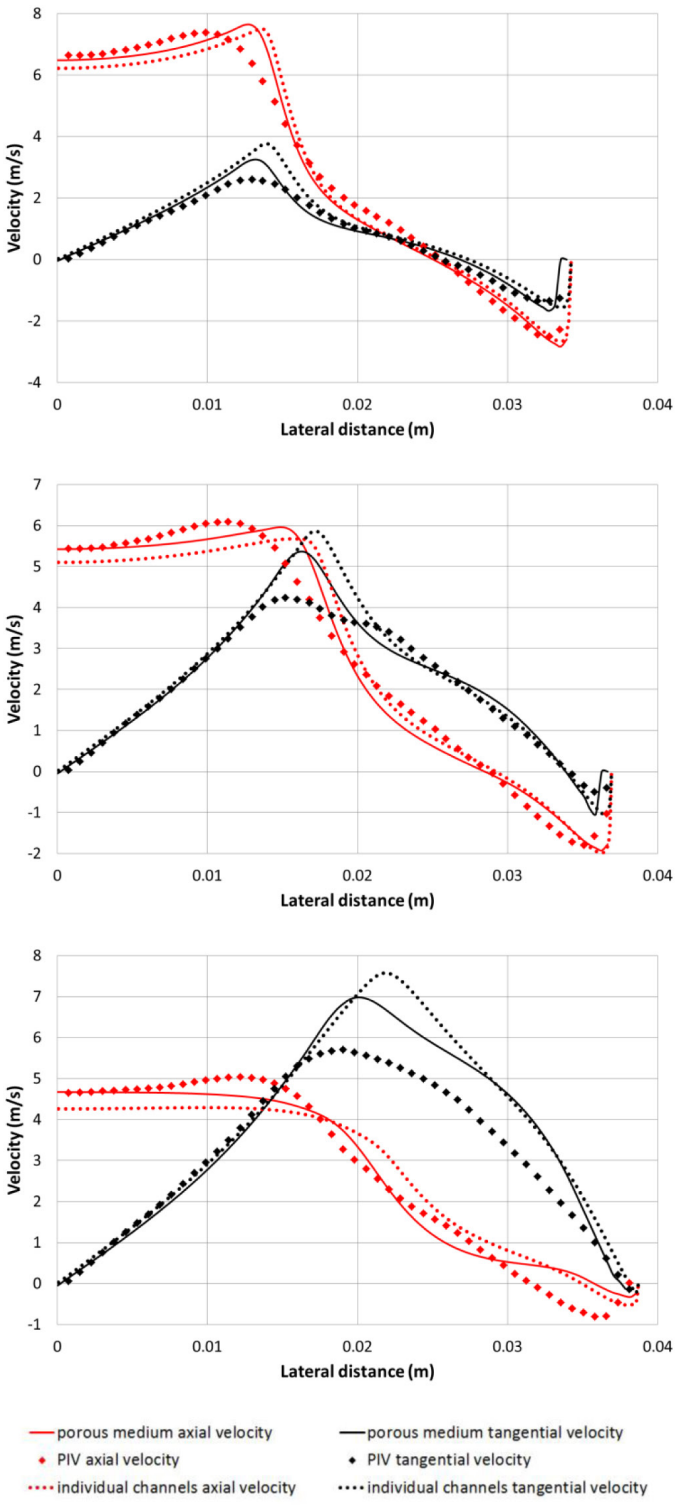

Figure 9. Axial and tangential velocity profiles 10.13mm (top), 5.55mm (centre) and 2.5mm upstream of 27mm monolith with inlet Re 2×10^4

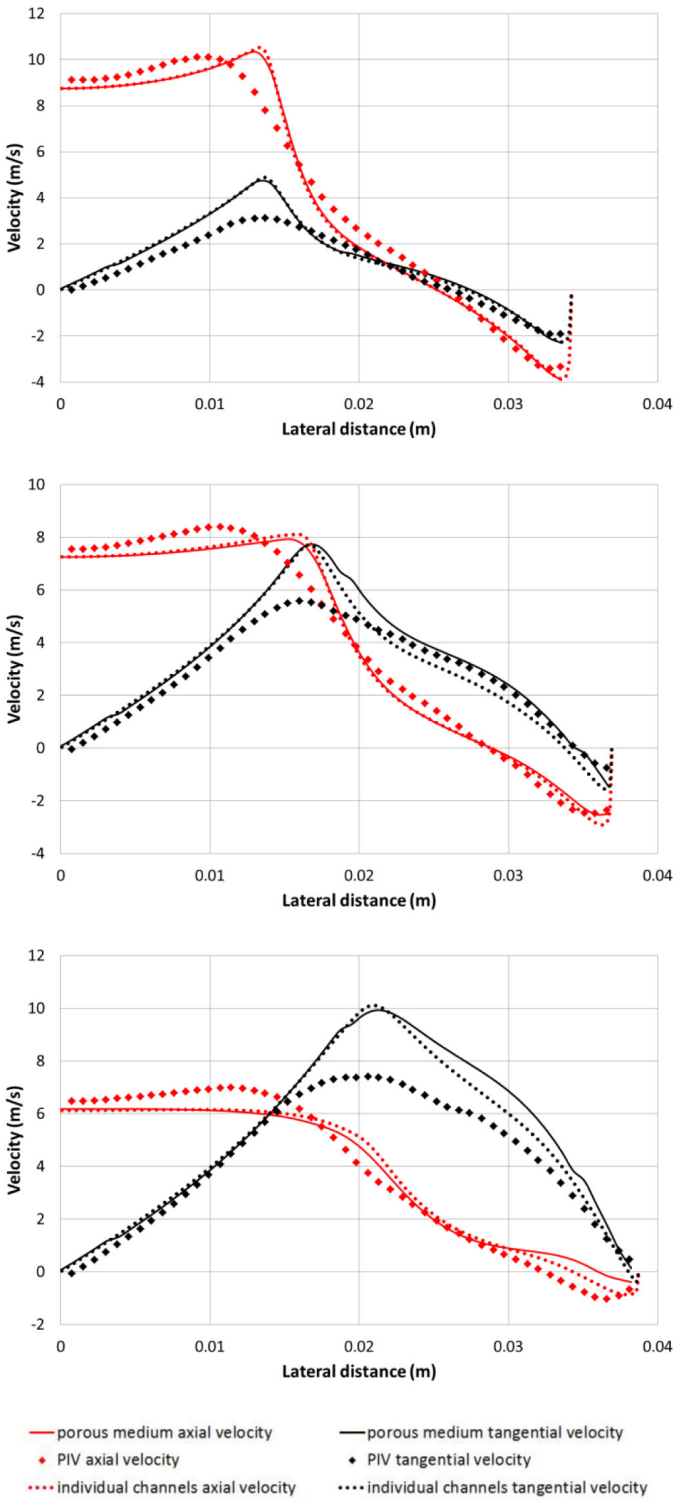

Figure 10. Axial and tangential velocity profiles 10.13mm (top), 5.55mm (centre) and 2.5mm upstream of 27mm monolith with inlet Re 3×10^4

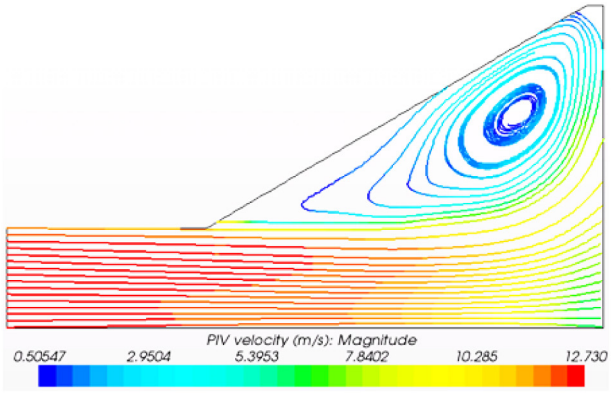

Figure 11. Velocity contour lines in diffuser interpolated from PIV data for 27mm monolith with inlet Re 3 × 10^4

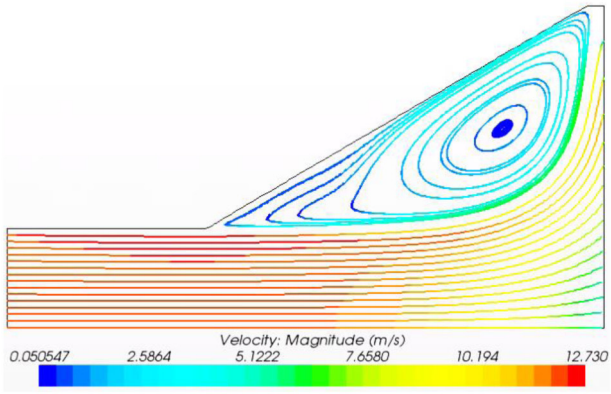

Figure 12. Velocity contours in diffuser from porous medium model for 27mm monolith with inlet Re 3 × 10^4

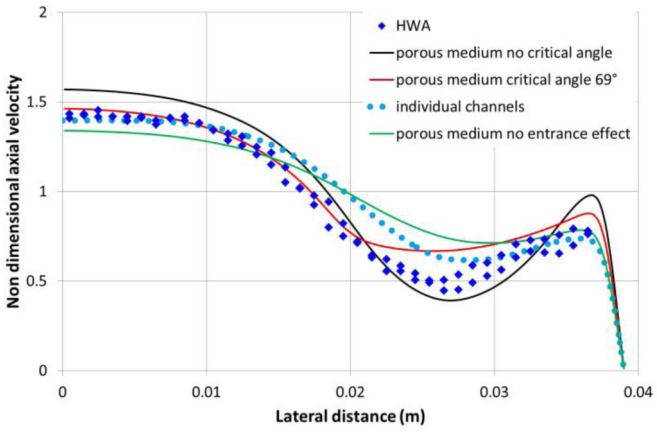

Figure 13. Non dimensional axial velocity profiles (u/Ū) 40mm downstream of 27mm monolith with inlet Re 2×10^4

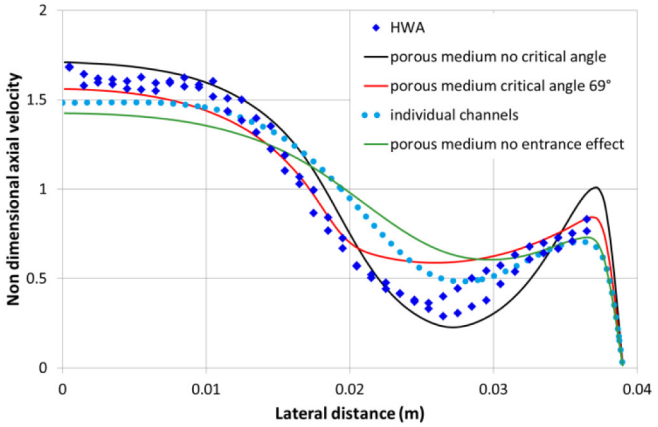

Figure 14. Non dimensional axial velocity profiles (u/Ū) 40mm downstream of 27mm monolith with inlet Re 3×10^4

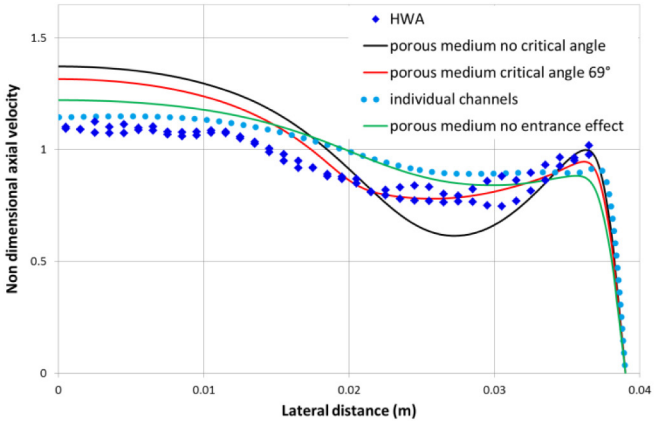

Figure 15. Non dimensional axial velocity profiles (u/Ū) 40mm downstream of 100mm monolith with inlet Re 2×10^4

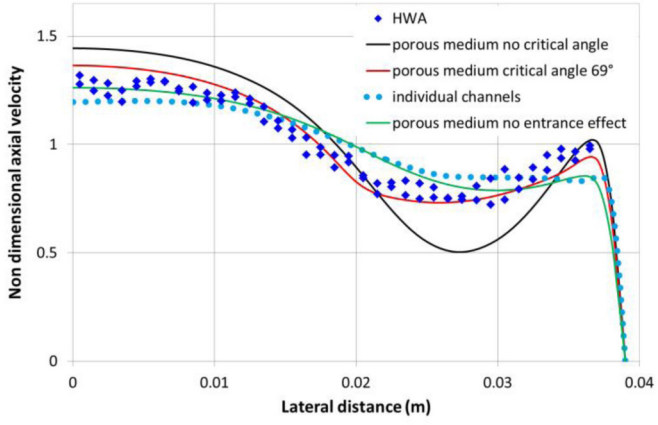

Figure 16. Non dimensional axial velocity profiles (u/Ū) 40mm downstream of 100mm monolith with inlet Re 3×10^4

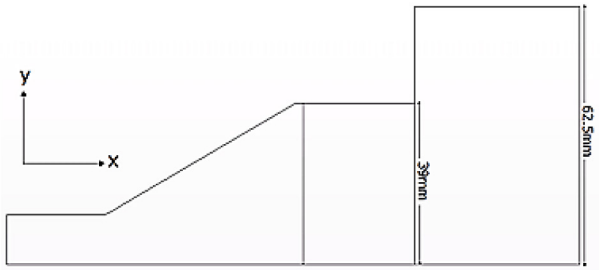

Figure 17. Geometry of 27mm monolith model with wide outlet sleeve

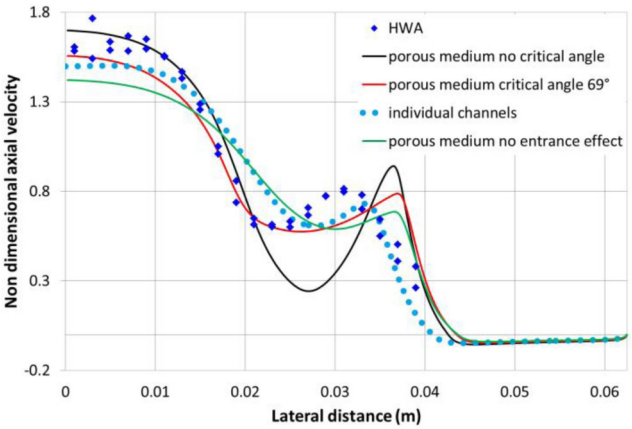

Figure 18. Non dimensional axial velocity profiles (u/Ū) 40mm downstream of 27mm monolith with inlet Re 3×10^4 for wide outlet sleeve

CONCLUSION

CFD studies have been performed for a catalytic converter system with a planar diffuser for steady flow. Two distinct approaches, porous medium and individual channels, have been used to model monoliths of length 27 mm and 100 mm with inlet flow of Re 2×10^4 and 3×10^4. Flow predictions were compared with each other and with particle image velocimetry measurements made in the diffuser and hot wire anemometry data taken downstream of the monolith. Both simulations compare favourably with PIV measurements although the models underestimate the degree of mixing in the shear layer at the periphery of the emerging jet. Tangential velocities are well-predicted in the central jet region but are overestimated elsewhere, especially at the closest measured distance, 2.5 mm from the monolith. The individual channels model is found to provide a more consistently accurate velocity profile downstream of the monolith. Maximum velocities, on the centre line and the secondary peak near to the wall, are reasonably well matched for the cases where the flow is more maldistributed. Under these conditions, a porous medium model remains attractive because of low computational demand.

REFERENCES

1. Benjamin, S.F., Haimad, N., Roberts, C.A. and Wollin, J., "Modelling the flow distribution through automotive catalytic converters," Proc. IMechE Part C 215, 2001.
2. Quadri, S.S., Benjamin, S.F. and Roberts, C.A., "An experimental investigation of oblique entry pressure losses in automotive catalytic converters," Proc. IMechE Part C, J. Mechanical Engineering Science 223:2561-2569, 2009, doi:10.1243/09544062JMES1565.
3. Persoons, T., Vanierschot, M. and Van den Bulck, E., "Oblique inlet pressure loss for swirling flow entering a catalyst substrate," Exp. Therm. Fluid Sci. 32:1223-1231, 2008.
4. Küchemann, D. and Weber, J., "Aerodynamics of propulsion," McGraw Hill, New York, 1953.
5. Breuer, M., Schernus, C., Böwing, R., Kuphal, A. et al., "Experimental Approach to Optimize Catalyst Flow Uniformity," SAE Technical Paper 2000-01-0865, 2000, doi:10.4271/2000-01-0865.
6. Turner, C., Thornhill, D., McCullough, G., and Patel, S., "Comparison of Experimental PIV Data and CFD Simulations for Flow in a Diesel Particulate Filter Inlet Diffuser," *SAE Int. J. Engines* 4(1):1556-1570, 2011, doi:10.4271/2011-01-1241.
7. Quadri, S.S., Benjamin, S.F. and Roberts, C.A., "Flow measurements across an automotive catalyst monolith situated downstream of a planar wide-angled diffuser," Proc IMechE Part C, J. Mechanical Engineering Science 224(2):321-328, 2009, doi: 10.1243/09544062JMES1735.
8. Mat Yamin, A.K., Benjamin, S.F. and Roberts, C.A., "Pulsating flow in a planar diffuser upstream of automotive catalyst monoliths," International Journal of Heat and Fluid Flow 40:43-53, 2013.
9. Mat Yamin, A.K., "Pulsating Flow Studies in a Planar Wide-angled Diffuser Upstream of Automotive Catalyst Monoliths," Ph.D. thesis, Coventry University, UK, 2012.
10. Cokljat, D., Kim, S.E., Iaccarino, G. and Durbin, P.A., "A comparative assessment of the V2F model for recirculating flows," presented at 41st Aerospace sciences Meeting and Exhibit, Reno, Nevada, USA, January 6-9, 2003, doi:10.2514/6.2003-765.

CONTACT INFORMATION

Automotive Engineering Applied Research Group, Faculty of Engineering and Computing, Coventry University, Priory Street, Coventry CV1 5FB, UK.
s.benjamin@coventry.ac.uk